HHS Public Access

Author manuscript

Mol Cancer Ther. Author manuscript; available in PMC 2018 January 24.

Published in final edited form as:

Mol Cancer Ther. 2017 June ; 16(6): 1102–1113. doi:10.1158/1535-7163.MCT-16-0314.

A Fas Ligand (FasL)-Fused Humanized Antibody Against Tumor-Associated Glycoprotein 72 Selectively Exhibits the Cytotoxic Effect Against Oral Cancer Cells with a Low FasL/Fas Ratio

Ming-Hsien Chien[1,2], **Wei-Min Chang**[3], **Wei-Jiunn Lee**[2,4], **Yu-Chan Chang**[3], **Tsung-Ching Lai**[3], **Derek V. Chan**[5], **Rahul Sharma**[5], **Yuan-Feng Lin**[1], and **Michael Hsiao**[3,6,7]

[1]Graduate Institute of Clinical Medicine, College of Medicine, Taipei Medical University, Taipei, Taiwan

[2]Department of Education and Research, Wan Fang Hospital, Taipei Medical University, Taipei, Taiwan

[3]The Genomics Research Center, Academia Sinica, Taipei, Taiwan

[4]Department of Urology, School of Medicine, College of Medicine, Taipei Medical University, Taipei, Taiwan

[5]Center for Immunity, Inflammation, and Regenerative Medicine, Department of Medicine, University of Virginia, Charlottesville, Virginia

[6]Department of Biochemistry, College of Medicine, Kaohsiung Medical University, Kaohsiung, Taiwan

[7]The PhD Program for Translational Medicine, College of Science and Technology, Taipei Medical University, Taipei, Taiwan

Abstract

Altered expression of the Fas ligand (FasL)/Fas ratio exhibits a direct impact on the prognosis of cancer patients, and its impairment in cancer cells may lead to apoptosis resistance. Thus, the development of effective therapies targeting the FasL/Fas system may play an important role in the

Corresponding Author: Yuan-Feng Lin, Graduate Institute of Clinical Medicine, College of Medicine, Taipei Medical University, 250 Wu-Hsing Street, Taipei 110, Taiwan. Phone: 8862-2736-1661, ext. 3106; Fax: 8862-2739-0500; d001089012@tmu.edu.tw; and Michael Hsiao, Genomics Research Center, Academia Sinica, 128 Academia Road, Taipei 11529, Taiwan. Phone: 8862-2787-1243; Fax: 8862-2789-9931; mhsiao@gate.sinica.edu.tw.

Note: Supplementary data for this article are available at Molecular Cancer Therapeutics Online (http://mct.aacrjournals.org/).

Disclosure of Potential Conflicts of Interest

No potential conflicts of interest were disclosed.

Authors' Contributions

Conception and design: M.-H. Chien, Y.-F. Lin, M. Hsiao

Development of methodology: W.-M. Chang, Y.-C. Chang, T.-C. Lai

Acquisition of data (provided animals, acquired and managed patients, provided facilities, etc.): M.-H. Chien, W.-M. Chang, W.-J. Lee, Y.-C. Chang, T.-C. Lai

Analysis and interpretation of data (e.g., statistical analysis, biostatistics, computational analysis): M.-H. Chien, Y.-F. Lin

Writing, review, and/or revision of the manuscript: M.-H. Chien, R. Sharma, Y.-F. Lin

Administrative, technical, or material support (i.e., reporting or organizing data, constructing databases): D.V. Chan, M. Hsiao

Study supervision: Y.-F. Lin, M.-H. Chien

Other (providing the reagents used in the study): R. Sharma

flght against cancer. In this study, we evaluated whether a fusion protein (hcc49scFv-FasL) comprising of the cytotoxicity domain of the FasL fused to a humanized antibody (CC49) against tumor-associated glycoprotein 72, which is expressed on oral squamous cell carcinoma (OSCC), can selectively kill OSCC cells with different FasL/Fas ratios. In clinical samples, the significantly low FasL and high Fas transcripts were observed in tumors compared with normal tissues. A lower FasL/Fas ratio was correlated with a worse prognosis of OSCC patients and higher proliferative and invasive abilities of OSCC cells. The hcc49scFv-FasL showed a selective cytotoxic effect on OSCC cells (Cal-27 and SAS) but not on normal oral keratinocytes cells (HOK) through apoptosis induction. Moreover, SAS cells harboring a lower FasL/Fas ratio than Cal-27 were more sensitive to the cytotoxic effect of hcc49scFv-FasL. Unlike wild-type FasL, hcc49scFv-FasL was not cleaved by matrix metalloproteinases and did not induce nonapoptotic signaling in SAS cells. *In vivo*, we found that hcc49scFv-FasL drastically reduced the formation of lymph node metastasis and decreased primary tumor growth in SAS orthotopic and subcutaneous xenograft tumor models. Collectively, our data indicate that a tumor-targeting antibody fused to the FasL can be a powerful tool for OSCC treatment, especially in populations with a low FasL/Fas ratio.

Introduction

Oral squamous cell carcinoma (SCC; OSCC) is the most commonly diagnosed malignancy of the oral cavity (1). Strategies used to treat OSCC include surgical extraction, radiotherapy, and chemotherapy either individually or in combination (2). Unfortunately, the prognosis is poor for relapsed and refractory disease and for patients with metastatic disease even after therapeutic interventions with chemotherapeutics, and the 5-year survival rate of patients with OSCC is around 50% which is very poor (2). It seems difficult to improve current response rates with further dose escalations to overcome drug resistance, as resistant tumor cells are able to withstand the effects of cytotoxic agents. In addition, associated cytotoxic side effects on normal tissues and organs remain a serious drawback. Therefore, searching for new and alternative therapeutic strategies such as targeted therapy has been the most essential and emergent issue.

Fas, a member of the TNF family, is a transmembrane protein with cysteine-rich extracellular domains and a death cytoplasmic domain, common to all family members and essential in the translation of the death stimulus. Immediately after receptor stimulation by the Fas ligand (FasL), an apoptotic signal is transmitted through the adapter Fas-associated death domain (FADD), which converts caspase-8 zymogen into its active form, triggering initiation of apoptosis (3). Recently, the FasL/Fas system was reported to elicit both tumorigenic and tumor-suppressive roles in the pathogenesis of cancer (4). FasL is expressed in two flavors, a membrane-bound form (mFasL) and a soluble form (sFasL), which is generated through cleavage of the mFasL by matrix metalloproteinases (MMP; refs. 5, 6). *In vivo*, the mFasL is essential for apoptosis induction, whereas the sFasL appears to promote tumorigenesis through nonapoptotic activities (7). For example, mice that only express sFasL but not mFasL suffer from large histiocytic sarcomas of the liver, and this sFasL-Fas–induced tumorigenic effect may be through inducing NFκB activation (7). More recently, sFasL was reported to trigger formation of a motility-inducing signaling complex in triple-negative breast cancer cells (8). To sensitize tumor cells to mFasL/Fas–mediated apoptosis,

various approaches have been developed to date (9). One promising approach is the development of FasL fusion proteins which harbor a protein domain that specifically recognizes tumor cells or tumor stroma antigens, which not only achieves immobilization of the ligand to the membrane, but enables tumor-restricted action of the system through specific binding to a tumor-associated antigen. For example, the sc40-FasL combines the extracellular domain of the FasL and a single-chain antibody fragment (scFv) that specifically recognizes the fibroblast-activating protein (FAP), a transmembrane protein restrictedly expressed during angiogenesis and on activated fibroblasts occurring in the stroma of epithelial cancer (10), thus acting as a tumor stroma marker. This fusion protein allows the specific immobilization of the FasL at FAP-expressing cells. Upon binding, the initially inactive protein converts into a protein with membrane-bound-FasL-like activity, specifically inducing apoptosis in FAP-expressing tumor cells both *in vitro* and *in vivo*, without triggering systemic toxicity (11). Along the same line, a FasL fusion protein (scFvCD7:sFasL) for CD7-restricted induction of apoptosis in T-cell leukemia was developed. As CD7 is an antigen associated with leukemia cells, it allows CD7-restricted induction of apoptosis (12).

The tumor-associated glycoprotein (TAG)-72 is a membrane protein complex of approximately 220–400 kDa (13). It was demonstrated that TAG-72 is overexpressed in a number of human tumors such as colon cancer, ductal breast cancer, lung cancer, epithelial ovarian cancer, hepatocellular carcinoma, and oral cancer, but is not expressed by most normal tissues (14–18). An anti-TAG-72 mAb (CC49) was studied in preclinical animal models and in humans for cancer detection based on its high specificity against cancer antigens in various solid cancers (17, 19). Herein, we investigated the anticancer effects on oral cancer *in vitro* and in tumor xenografts using our synthesized fusion protein, hcc49scFv-FasL (20), which is comprised of the extracellular cytotoxic domain of the FasL fused to a humanized TAG-72 antibody, CC49.

We found that the FasL/Fas ratio in OSCC cells was inversely correlated with the *in vitro* proliferative and invasive abilities and *in vivo* tumor growth rate, and positively correlated with the clinical prognosis of OSCC patients. We demonstrate that the recombinant hcc49scFv-FasL selectively induces apoptosis of OSCC cells (Cal-27 and SAS), but not normal oral keratinocytes. Interestingly, cells harboring a lower FasL/Fas ratio, such as SAS, presented higher sensitivity to hcc49scFv-FasL treatment compared with cells harboring a higher FasL/Fas ratio, such as Cal-27. *In vivo*, the hcc49scFv-FasL dramatically inhibited tumor growth through apoptosis induction in SAS subcutaneous and orthotopic graft models through intratumoral and intraperitoneal (i.p.) administration, respectively. In addition, intraperitoneal administration of the hcc49scFv-FasL strongly limited the formation of metastasis to neck lymph nodes and prolonged survival times in the orthotopic metastatic mouse model.

Materials and Methods

Reagents

A recombinant hcc49scFv-FasL was generated according to our previous report (20). The recombinant FasL, MMP7, and pro-form SPP1 (Osteopontin) proteins were purchased from

(R&D Systems). Antibodies against phospho-p38 (9211), p38 (9212), phospho-extracellular signal-regulated kinase (ERK)1/2 (9101), Erk1/2 (9102), phospho-NFκB-p65 (3036), NFκB-p65 (3034), phospho-I-κB (9246), I-κB (4818), pro-caspase-3 (9662), cleaved caspase-3 (9661), and Snail (3895) were obtained from Cell Signaling Technology. Antibodies against Fas (GTX116024) and FasL (GTX116044) were purchased from Genetex. An antibody specific for N-cadherin (610921) was purchased from BD Biosciences. An antibody against α-tubulin (T5168) was purchased from Sigma. An antibody neutralized Fas activity (05-338) was purchased from Merck Millipore. 3-(4,5-Dimethylthiazol-2-yl)-2,5-diphenyl tetrazolium bromide (MTT) powder was purchased from Sigma.

Processing of microarray data from GEO database

Microarray datasets with accession number GSE42743 and GSE13601 were obtained from Gene Expression Omnibus (GEO) database and normalized by GeneSpring (Agilent Technologies) software as log2 values.

Cell culture

The OSCC lines Cal-27, Detroit-562, and RPMI-2650 were obtained from ATCC and cultured in modified Eagle medium (MEM) containing 10% FBS, 2 mmol/L L-glutamine and 100 U/mL penicillin. HSC-4 and SAS cell lines were obtained from Japanese Collection of Research Bioresources (JCRB) Cell Bank and cultured in MEM and DMEM, respectively, supplemented with the same additives. Human lung epithelial cell line WI-38 was obtained from Bioresource Collection and Research Center (BCRC; Hsinchu, Taiwan) and cultured in MEM with 10% FBS, 2 mmol/L L-glutamine, 0.1 mmol/L nonessential amino acids, 1.0 mmol/L sodium pyruvate, and 100 U/mL penicillin. Human oral keratinocytes (HOK) cells were purchased from ScienCell and cultured in oral keratinocyte medium (catalog no. 2611, Scien-Cell). Cells were incubated in 5% CO_2 at 37°C. All components used for cell cultures were purchased from Gibco (Invitrogen). All cells were routinely authenticated on the basis of morphologic and growth characteristics as well as by STR analysis and confirmed to be free of mycoplasma.

Establishment of red fluorescence protein (DsRed2)-expressing SAS cells

The *DsRed2* gene was cloned into the pDsRed2-C1 vector (Clontech) with *Eco*RI and *Not*I and then subcloned into the pCI-Neo expression vector with the same restriction enzymes. SAS cells were transfected with pCI-DsRed2-Neo by calcium phosphate transfection reagent (Invitrogen). DsRed2-expressing SAS cells were further selected in the presence of 800 μg/mL neomycin. SAS-DsRed2 cells were maintained with the condition medium in the presence of 200 μg/mL neomycin.

Crispr/Cas9–mediated knockout of Fas and FasL in OSCC cells

All-in-one Cas9-sgRNA lentiviral expression Crispr nuclease vector were obtained from RNAiCore facility (Academia Sinica, Taipei, Taiwan). The FAS (GGAGTTGATGTCAGTCACTT) and FASLG (AAGTGACTGACATCAACTCC) sgRNA sequences were designed by using E-Crispr design algorithm and synthesized as a double-

strand DNA prior to clone into Cas9-sgRNA expression vector according the manufacturer's guidelines. All of the constructs were verified via double-strand plasmid sequencing. The control (no-sgRNA) and the Crispr knockout pseudovirus particles were done by following the standard protocol from RNAiCore facility. Cells were infected with designated pseudovirus particles with the incubation for 48 hours and then selected with 10 μg/mL puromycin for another 48 hours. The single-cell dilution was performed to obtain the successful Crispr knockout cells and verified by Sanger DNA sequencing against the specific sgRNA targeting genomic DNA regions.

Real-time PCR assay

mRNA was isolated and amplified as described previously (20). The real-time PCR experiments for FAS and FASLG were performed by using paired primers (for FAS: forward primer_5′-TCTGGTTCTTACGTCTGTTGC-3′, reverse primer_5′-CTGTGCA-GTCCCTAGCTTTCC-3′; for FASLG: forward primer_5′-CTCCGA-GAG TCTACCAGCCA-3′, reverse primer_5′-TGGACTTGCCTGT-TAAATGGG-3′).

Western blot analysis

Protein lysates were prepared as described previously (20). A Western blot analysis was performed with primary antibodies for phospho-p38, p38, phospho-ERK1/2, ERK1/2, phospho-JNK, JNK, phospho-NFκB-p65, NFκB-p65, pro-caspase-3, cleaved cas-pase-3, N-cadherin, Snail, or α-tubulin.

Cytotoxicity assay

Cells (2×10^3) were seeded in wells of a 96-well plate. After 24 hours, medium was replaced with 200 μL fresh medium containing various dosages of the hcc49scFv-FasL (50, 25, 12.5, 6.25, and 3.125 μg) for 72 hours. At the end point, 100 μL of an MTT (1 mg/mL in PBS) solution was added to the cell culture. After a 4-hour incubation, media were removed, and 200 μL of DMSO plus 25 μL of glycine buffer (0.1 mol/L glycine and 0.1 mol/L NaCl, pH 10.5) was added to each well to dissolve the cellular crystals of MTT. The optical density of MTT at 540 nm was detected by an ELISA plate reader (Anthos).

TUNEL assay

Cells were grown on glass cover slides in 6-well plates. Cells were fixed with 4% paraformaldehyde for 1 hour and further incubated with permeabilization solution (sodium citrate buffer containing 0.1% of Triton X-100) for 2 minutes. For formalin-fixed, paraffin-embedded (FFPE) cases, samples were deparaffinized using xylene and rehydrated in a graded series of ethanol with a final wash in tap water. Antigen retrieval was treated with Target Retrieval Solution (DAKO). After a PBS wash, terminal deoxynucleotidyl transferase deoxyuridine triphosphate nick end labeling (TUNEL) reaction mixtures were applied to whole samples in the dark at 37°C for 1 hour. A DAPI solution (Vector Laboratories) was used to stain nuclei for 5 minutes before sealing on a slide for observation by fluorescence microscopy.

Transwell invasion assay

The invasion assay was performed using Transwell inserts for a 24-well plate that contained 8-μm pores (Corning Costar). OSCC cells plated in a Matrigel (BD Biosciences) coated top chamber and incubated for 24 hours. The numbers of cells that invaded were normalized to the growth rate for each cell line.

Animal model

SAS-DsRed2 cells were collected and diluted to 5×10^7 cells/mL in PBS. Each mouse was injected subcutaneously with 100 μL of the cell suspension on both rear sides or orthotopically with 20 μL of a cell suspension into buccal tissues under anesthesia. The hcc49scFv-FasL recombinant protein at designated concentrations was applied by an intratumoral injection into a subcutaneous tumor twice daily or by an intraperitoneal injection in the orthotopic experiment. Tumor growth was measured with a caliper or fluorescent in vivo imaging system (Kodak). The length (L) and width (W) of the tumor were measured with a caliper every week, and the tumor volume (TV) was calculated as TV (mm^3)= ($L \times W^2$)/2. Tumor metastasis was observed by fluorescent *in vivo* imaging system. After the mice were sacrificed, organs and primary tumors were recorded with fluorescent stereomicroscope (Olympus). Tissues were fixed with fixation solution (10% formalin, 5% glacial acetate, and 72% ethanol), dehydrated, and embedded in paraffin blocks. All animal procedures were approved by the Institutional Animal Care and Use Committee at Academia Sinica (Taipei, Taiwan).

Hematoxylin and eosin staining

Tissue samples were set in a 60°C oven for 1 hour, and then sequentially soaked in xylene, 100% EtOH, 95% EtOH, 75% EtOH, 50% EtOH, and 30% EtOH prior to performing hematoxylin staining for 5 minutes. After a wash with tap water for 5 minutes, samples were incubated with an eosin solution for 1 minute and then sequentially dipped into 75% EtOH, 95% EtOH, 100% EtOH, and xylene. Finally, samples were mounted with mounting solution (DAKO).

Statistical analysis

Each experiment was repeated three times. The values are presented as the means ± SE. The statistical analysis was performed using Statistical Package for Social Science software, version 16 (SPSS). When two groups were compared, the data were analyzed using Student t test. A one-way ANOVA followed by Tukey *post hoc* test was used to analyze three or more groups. Statistical analyses of the correlation between FasL/Fas ratio and proliferation or invasiveness of OSCC cells were performed with the Spearman rank correlation analysis; P values of < 0.05 were considered statistically significant.

Results

A low FasL/Fas ratio is associated with tumorigenesis and predicts a poorer prognosis in patients with OSCC

To examine FasL and Fas expressions in patients with OSCC, 74 OSCC cases were analyzed from the Gene Expression Omnibus (GEO) database (GSE42743). Significantly low FasL and high Fas transcripts were observed in tumors compared with normal tissues (Fig. 1A). Moreover, an analysis of 40 matched tumor tissues and their corresponding normal tissues (GSE13601) revealed lower FasL and higher Fas expressions in the tumors (Fig. 1B). The Kaplan–Meier plot revealed a favorable overall survival of patients with high FasL expression ($P = 0.037$; Fig. 1C). Relationships between the level of FasL/Fas expression and the prognosis of OSCC patients are shown in Fig. 1D. Most importantly, patients who had $FasL^{low}/Fas^{high}$ tumors had shorter survival times compared with those who had $FasL^{high}/Fas^{low}$ tumors. Taken together, the above clinical data indicate that downregulation of the FasL/Fas ratio is a critical event in promoting OSCC progression.

Effect of the FasL/Fas ratio on the proliferative abilities of OSCC cells *in vitro* and *in vivo*

The clinical findings suggested that the FasL/Fas ratio may affect the proliferative ability of oral cancer cells. We next evaluated the correlation between the FasL/Fas ratio and the cell proliferative ability, because OSCC is the most common malignant tumor of the head and neck. First, we used a set of head and neck SCC cell lines including Cal-27, HSC-4, SAS, Detroit-562, and RPMI-2650 to investigate expression levels of the FasL (Fig. 2A) and Fas (Fig. 2B) using a quantitative PCR. Next, proliferation rates of these cell lines were monitored in real time with the IncuCyte Life-Cell Imaging System (Fig. 2C). We observed that SAS cells expressed the lowest and highest levels of the FasL and Fas, respectively, in these cell lines (Fig. 2A and B) and also exhibited the highest proliferative index among these cell lines (Fig. 2C). To further compare the correlation between the FasL/Fas ratio and the proliferative index among these cell lines, we found a nonsignificant trend toward an inverse correlation (Spearman rank correlation coefficient $\rho = -0.863$, $P = 0.078$) between the FasL/Fas ratio and proliferative abilities of these cell lines (Fig. 2D). We next examined the *in vivo* effects of the FasL/Fas ratio on tumor growth. Five head and neck SCC cells were subcutaneously injected into BALB/c nude mice, and we found that SAS-injected mice formed larger tumors than those in mice injected with other SCC cells after 3 weeks (Fig. 2E). These data suggest that altered expression of the FasL/Fas ratio in OSCC might be important for influencing tumor growth *in vitro* and *in vivo*.

Significant and selective antiproliferative effects of the hcc49scFv-FasL fusion protein in OSCC cells

In our previous study, we developed the hcc49scFv-FasL fusion protein which can specifically target the tumor antigen, TAG-72, and showed it to be 30,000-fold more cytotoxic against $TAG\text{-}72^{+}$ Jurkat lymphoma cells compared with sFasL treatment (20). TAG-72 was also found to be expressed by oral cancer cells (18, 21), indicating that hcc49scFv-FasL, possibly through binding to TAG-72, induced FasL-mediated cell death (Fig. 3A). To determine the *in vitro* efficacy of the hcc49scFv-FasL in OSCC cells, the cytotoxic effects of hcc49scFv-FasL were examined in two OSCC cell lines (SAS and

CaL-27) which represent different FasL/Fas ratios. As shown in Fig. 3B, the cytotoxicity of hcc49scFv-FasL toward SAS, CaL-27, and normal cell lines, NHOK (normal human oral keratinocytes), and WI38 cells (human lung fibroblast cells) at various concentrations (0–50 μg/mL) for 72 hours were determined by an MTT assay. The results showed that hcc49scFv-FasL exhibited much more potent cytotoxicity against the OSCC cell lines than normal cells especially cells (SAS) with a lower FasL/Fas ratio (Fig. 3B). Compared with hcc49scFv-FasL, wild-type FasL did not show different cytotoxic effects on NHOK and SAS cells (Fig. 3C). To investigate the mode of cell death induced by hcc49scFv-FasL, SAS cells were treated with hcc49scFv-FasL (50 μg/mL) for 72 hours and then subjected to a TUNEL assay. Nuclei of hcc49scFv-FasL–treated cells were small, condensed, and TUNEL positive, suggesting apoptosis was induced by hcc49scFv-FasL (Fig. 3D). The NFκB and MAPK signaling pathways were shown to control the cell proliferation and apoptosis of a great variety of cancers (22, 23). Moreover, sFasL stimulation in cancer cells can induce nonapoptotic events such as motility and invasiveness promotion through activating ERK and NFκB signaling pathways (24, 25). We therefore examined the effect of hcc49scFv-FasL on the MAPKs and NFκB pathways in OSCC cells. Our results showed that treatment of SAS cells with hcc49scFv-FasL (50 μg/mL) for different time points (0, 1, 6, and 24 hours) induced activation of caspase-3 and suppressed activation of ERK1/2 and NFκB (Fig. 3E), suggesting that hcc49scFv-FasL did not turn on the nonapoptotic signaling and suppression of NFκB and ERK pathways might be involved in hcc49scFv-FasL–mediated cell apoptosis in OSCC cells.

Significant antitumorigenic effect of hcc49scFv-FasL in SAS subcutaneous and orthotopic graft models

We next examined the *in vivo* effects of hcc49scFv-FasL on tumor growth. Previous reports showed that transduction and expression of fluorescent proteins in cancer cells can be used for real-time tracking of cells in mouse internal organs and does not affect cell behaviors such as metastasis (26–28). Here, DsRed2-expressing SAS cells were established, subcutaneously injected into BALB/c nude mice, and allowed to become stable for 3 days before initiating treatment. SAS-DsRed2 graft mice were directly intratumorally injected with hcc49scFv-FasL (1 mg) or vehicle control twice daily, and tumor growth was monitored by fluorescent light imaging. Figure 4A shows the dominant inhibitory effect of hcc49scFv-FasL on tumor growth after 10 days of treatment by *in vivo* fluorescent detection. Next, we examined the effects of hcc49scFv-FasL on cell apoptosis within SAS tumors after 10 days of treatment. The number of TUNEL-positive cells had dramatically increased in hcc49scFv-FasL–injected tumors compared with vehicle-injected tumors (Fig. 4B). Moreover, we also established SAS-DsRed2 orthotopic graft mice, and 3 days after cells were injected, we treated mice with the hcc49scFv-FasL (1 mg) or the vehicle control every day by intraperitoneal administration for 5 or 10 days. Tumor growth inhibition was also observed after injecting tumor cells for 2 and 4 weeks (Fig. 4C).

The FasL/Fas ratio is inversely correlated with the invasive abilities of OSCC cells and significant antimetastatic effects of the hcc49scFv-FasL in a SAS orthotopic graft model

In addition to the effects of the FasL/Fas ratio on the proliferation of OSCC cells, we further investigated the correlation between the FasL/Fas ratio and cell invasive ability. We first

evaluated the invasive abilities of five head and neck SCC cell lines (Cal-27, HSC-4, SAS, Detroit-562, and RPMI-2650) by a transwell invasion assay and found a variety of invasive abilities among these cell lines, with SAS cells exhibiting the highest invasive ability (Fig. 5A). We combined this result with the results from Fig. 2A and B and found a significant inverse correlation (Spearman rank correlation coefficient $\rho = -0.9$, $P = 0.037$) between the FasL/Fas ratio and the invasive abilities of these cell lines (Fig. 5B). A previous report indicated that sFasL can induce epithelial–mesenchymal transition (EMT) to promote motility of gastrointestinal cancer (24). We next evaluated the *in vitro* effects of the hcc49scFv-FasL on tumor-invasive ability. In contrast to sFasL, hcc49scFv-FasL can suppress invasion of SAS cells by inhibiting expression of mesenchymal markers, N-cadherin and Snail (Fig. 5C and D). Furthermore, we examined the *in vivo* effects of the hcc49scFv-FasL on tumor metastasis. SAS-DsRed2 cells were orthotopically injected into BALB/c nude mice for 3 days, and then mice were treated with the hcc49scFv-FasL (1 mg) or the vehicle control every day by intraperitoneal administration for 5 days. Figure 5E shows that the formation of spontaneous cervical lymph nodes metastasis was dramatically prevented by the hcc49scFv-FasL according to evidence from *in vivo* and *ex vivo* fluorescent imaging 6 weeks after injecting tumor cells. In addition, hematoxylin and eosin (H&E) staining revealed a prevention of cervical lymph node tumor metastasis in response to hcc49scFv-FasL treatment (Fig. 5F). Most importantly, mice with tumors and hcc49scFv-FasL treatment had significantly longer survival times compared with mice with tumors and vehicle treatment (Fig. 5G). Together, these results revealed that hcc49scFv-FasL treatment suppressed invasion and lymph node metastasis of OSCC *in vitro* and *in vivo*, respectively.

The *in vitro* and *in vivo* antitumor effects of hcc49scFv-FasL rely on endogenous Fas receptor in OSCC cells

To prove the antitumor effects of hcc49scDv-FasL were relying on endogenous Fas receptor, we preformed the Crispr knockout system on endogenous Fas of SAS cells. The deletion mutants with early translational termination codon were identified in two alleles of Fas Crispr knockout SAS cells (Fig. 6A; Supplementary Fig. S1A). The Fas Crispr knockout appeared to completely deplete the endogenous Fas expression (Fig. 6B), abolish the tumoricidal effects of hcc49scDv-FasL *in vitro* and *in vivo* (Fig. 6C–F), prevent the proteolytic activation of caspase-3, and restore the phosphorylation of ERK1/2, p38, IκB, and NFκB (Fig. 6G) in SAS cells. Accordingly, the neutralization of Fas with its specifically blocking antibody was also capable of relieving cell death (Supplementary Fig. S2A), preventing caspase-3 cleavage (Supplementary Fig. S2B) and rescuing the phosphorylation of ERK1/2, p38, IκB, and NFκB (Supplementary Fig. S2C) in the hcc49scDv-FasL–treated SAS cells. In contrast, the Crispr knockout of FasL (Supplementary Fig. S3A and S3B) enhanced the apoptotic cell death in Cal-27 cells posttreatment with hcc49scDv-FasL (Supplementary Fig. S3C and S3D). Taken together, our results showed that the antitumor function of hcc49scDv-FasL heavily relies on endogenous Fas receptor in OSCC cells and the FasL/Fas ratio determines the antitumor effectiveness of hcc49scDv-FasL.

Discussion

The extrinsic apoptosis pathway can be triggered by enzymes of the TNF family, including Fas and the FasL. FasL-positive T cells can eliminate Fas-positive tumoral cells by inducing apoptosis (29). Fas is expressed by almost all human tumor cells including oral cancers (30, 31); however, given the fact that almost all established cancers express Fas, most cancer cells are resistant to apoptosis induction (4). This is because increased amounts of the sFasL are produced by MMP-mediated cleavage of extracellular domains of the mFasL and are released by these apoptosis-resistant cancer cells (5). The sFasL enables a powerful "counterattack" against antitumor immune effector cells, such as cytotoxic T cells, resulting in a repressed tumor attack by the immune system, and this phenomenon was also observed in head and neck cancers (32–34). Actually, higher concentrations of sFasL in the serum of many cancer patients (4) may be interpreted as the context of sFasL counterattack theory. Moreover, previous reports also indicated that altered FasL and Fas expressions by peripheral blood T cells as well as FasL- and Fas-mediated apoptosis of the major T-cell subsets are possible mechanisms for the down-regulation of immune functions and reduced apoptosis of tumor cells in patients with tobacco-related OSCC (35, 36). According to these results, the major cause of cancer cell resistance to Fas-mediated apoptosis is the FasL aimed at the wrong target.

An alternative strategy to overcome these limitations is to develop a novel Fas agonist with high sensitivity and specificity for cancer cells. In this respect, we generated a FasL fusion protein (20) and selected the anti-TAG-72 antibody as a fusion partner due to its specific binding ability to the TAG-72 antigen in tumors, including oral cancer (18). Anti-TAG-72 mAbs were studied in preclinical animal models and in humans for cancer detection based on their high specificity against cancer antigens in various solid cancers. For example, the anti-TAG-72 antibody was used as a radioimmunotherapeutic agent to treat ovarian cancer (37). Moreover, several nanoparticles conjugated with the anti-TAG-72 antibody were also used as targeting agents for radioimmunotherapy and tumor imaging (13, 38). The CC49 mAb recognizes the sialyl-Tn and sialyl-T epitopes, which are disaccharide carbohydrate antigens present on TAG-72. This antibody showed better immunoreactivity compared with other TAG-72–reactive antibodies in tumors (19). Hence, we investigated the anticancer effects of the fusion protein hcc49scFv-FasL of the extracellular cytotoxic domain of the FasL fused to a humanized antibody, CC49, on oral cancer. We found that the hcc49scFv-FasL, but not recombinant sFasL, exhibited higher cytotoxicity and a greater apoptosis-inducing effect on OSCC cells compared with normal oral keratinocytes and lung fibroblasts, suggesting the problem of wrong targeting by the FasL can be improved. Although we did not test the cytotoxic effect of the hcc49scFv-FasL on primary T cells, it was demonstrated that TAG-72 is not expressed by T cells (39). We assumed that the hcc49scFv-FasL might also exhibit lower sensitivity to cytotoxic T cells than cancer cells.

The wild-type FasL can be cleaved from the cell surface by MMPs and accumulates as an sFasL (40). It was observed that sFasL can have proapoptotic and antiapoptotic functions depending on the local microenvironment (5, 40). The sFasL can induce apoptosis following association/aggregation with ECM proteins or after spontaneous aggregation (40, 41). However, the antiapoptotic function is mediated by sFasL that competes with mFasL for Fas

binding. The sFasL exists as a homotrimer, which is ineffective at coaggregating Fas. Therefore, its interaction with the receptor results in null signaling and a lack of apoptosis (5). A previous report indicated that nonapoptotic signaling through Fas in cancer cells involved activation of NFκB and MAPKs (24, 25). Our results showed that treatment of OSCC cells with the hcc49scFv-FasL only induced activation of the caspase-3, but not the NFκB or MAPK pathway, suggesting that the hcc49scFv-FasL might not induce Fas-mediated nonapoptotic signaling in OSCC cells. Moreover, the hcc49scFv-FasL–mediated apoptotic effect was also observed in an OSCC xenograft model. Furthermore, the metalloprotease ADAM10 was reported to be the major protease responsible for generating sFasL ectodomain to suppress inflammatory response (42). According to the map of the FasL, we constructed (Supplementary Fig. S4A), the ADAM10 cleavage site was not included in this construct, suggesting that the hcc49scFv-FasL might not be cleaved by ADAM10. Taken together, our results indicated that the hcc49scFv-FasL is an effective apoptosis-inducing agent that inhibited the growth of OSCC tumors *in vitro* and *in vivo* by selectively and tightly binding with cancer cells.

In addition to Fas-mediated nonapoptotic signaling in cancer cells, a previous report also indicated that sFasL or mFasL can induce Fas-mediated invasiveness of cancer cells such as breast and ovarian cancers. Activation of NFκB, ERK, and the urokinase plasminogen activator (uPA) or expression of mesenchymal markers, N-cadherin and Snail was reported to play critical roles in the Fas-mediated invasiveness of cancer cells (24, 25). In the current study, hcc49scFv-FasL suppressed the NFκB or ERK activation and N-cadherin or Snail expression in OSCC cells and prevented the invasive ability *in vitro* and neck lymph node metastasis in an orthotopic graft model, and as a consequence, it prolonged the survival times of mice with OSCC. The aforementioned data indicated that the hcc49scFv-FasL might functionally differ from sFasL and mFasL which have an invasion-inducing effect in cancers. Moreover, orthotropic implantation of patient-derived intact tumor tissue in immunocompromised mice was reported to closely mimic the clinical pattern of metastasis (43). Furthermore, as uPA is a well-established NFκB target gene (44), our future experiments will address the effect of the hcc49scFv-FasL on aforementioned xenograft model and uPA expression and activation.

Chemotherapeutic drugs are the most frequently used apoptosis inducers in OSCC. Several previous reports indicated that FasL/Fas signaling plays a critical role in chemoresistance to doxorubicin and oxaliplatin by interacting with MMP-7 (45, 46). The chemotherapeutic drug-induced upregulation of MMP-7 can generate tumor-derived sFasL by cleavage of its membrane form and further counteract the host immune system by eliminating Fas-sensitive cytotoxic T cells (34, 45, 46). Actually, according to immunohistochemical staining results of esophageal squamous cell carcinoma (ESCC), FasL expression was diffusely observed in stromal cells around ESCC cells following chemoradiotherapy (CRT), supporting the CRT-induced sFasL counterattack theory (47). In the current study, we incubated recombinant hcc49scFv-FasL or osteopontin (SPP1) with purified active MMP-7 *in vitro*. SPP1 was used as a positive control for MMP-7 cleavage (48). We found that only the SPP1, but not hcc49scFv-FasL, was cleaved by MMP-7 (Supplementary Materials and Methods and Supplementary Fig. S4B), suggesting that a combination of chemotherapy and hcc49scFv-FasL (specifically targeting Fas on cancer cells) may be beneficial for OSCC treatment.

In conclusion, our study shows that increased FasL/Fas expression ratio correlated with favorable prognoses in OSCC patients and worse proliferative and invasive abilities of OSCC cells. We clearly demonstrated that fusing the CC49 antibody to the extracellular cytotoxic domain of the FasL is a promising approach for suppressing tumor growth and metastasis of OSCC cells, especially cells harboring a low FasL/Fas expression ratio. This fusion protein exhibited powerful tumor-targeting and tumor-binding abilities because of the anti-TAG-72 antibody and no MMP cleavage sites within the extracellular domain of the FasL. Moreover, the tumor-promoting signals of Fas cannot be turned on by this fusion protein. Previous reports indicated that labeling of nucleus and cytoplasm of cancer cells with different fluorescent proteins or tumor cells expressing DsRed2 are implanted in mice transgenic for green fluorescence are suitable models to, respectively, observe the nuclear–cytoplasmic dynamics and tumor–host interactions *in vivo* (49, 50). Our future works will try to use these models to further investigate the diverse anticancer effects of hcc49scFv-FasL *in vivo*. Moreover, a detailed preclinical drug safety analysis will be required to further assess the promise of this fusion protein. Taken together, the hcc49scFv-FasL fusion protein provides a novel approach to developing death receptor–targeting anti-cancer therapeutics, which merit additional investigation.

Supplementary Material

Refer to Web version on PubMed Central for supplementary material.

Acknowledgments

We would like to thank Dr. Shyr-Te Ju for help and advice on hcc49scFv-FasL fusion protein.

Grant Support

This study was supported by a grants (NSC102-2320-B-038-038-MY3) from the National Science Council of Taiwan (to M.H. Chien) and (MOST104-2320-B-038-010- MY2 and MOST 104-2320-B-038-061-MY3) from the Ministry of Science and Technology (to Y.F. Lin). This study was supported by Academia Sinica and Ministry of Science and Technology grants MOST 104-0210-01-09-02, MOST 105-0210-01-13-01, and MOST-406-0210-01-15-02 to M. Hsiao. This study was also supported by grants (1R01DK105833 and 2R01AI116725 to R. Sharma from National Institutes of Health.

References

1. Bagan JV, Scully C. Recent advances in Oral Oncology 2007: epidemiology, aetiopathogenesis, diagnosis and prognostication. Oral Oncol. 2008; 44:103–8. [PubMed: 18252251]
2. Rapidis AD, Gullane P, Langdon JD, Lefebvre JL, Scully C, Shah JP. Major advances in the knowledge and understanding of the epidemiology, aetiopathogenesis, diagnosis, management and prognosis of oral cancer. Oral Oncol. 2009; 45:299–300. [PubMed: 19411038]
3. Ashkenazi A, Dixit VM. Apoptosis control by death and decoy receptors. Curr Opin Cell Biol. 1999; 11:255–60. [PubMed: 10209153]
4. Peter ME, Hadji A, Murmann AE, Brockway S, Putzbach W, Pattanayak A, et al. The role of CD95 and CD95 ligand in cancer. Cell Death Differ. 2015; 22:549–59. [PubMed: 25656654]
5. Schneider P, Holler N, Bodmer JL, Hahne M, Frei K, Fontana A, et al. Conversion of membrane-bound Fas(CD95) ligand to its soluble form is associated with downregulation of its proapoptotic activity and loss of liver toxicity. J Exp Med. 1998; 187:1205–13. [PubMed: 9547332]
6. Tanaka M, Itai T, Adachi M, Nagata S. Downregulation of Fas ligand by shedding. Nat Med. 1998; 4:31–6. [PubMed: 9427603]

7. O'Reilly LA, Tai L, Lee L, Kruse EA, Grabow S, Fairlie WD, et al. Membrane-bound Fas ligand only is essential for Fas-induced apoptosis. Nature. 2009; 461:659–63. [PubMed: 19794494]
8. Malleter M, Tauzin S, Bessede A, Castellano R, Goubard A, Godey F, et al. CD95L cell surface cleavage triggers a prometastatic signaling pathway in triple-negative breast cancer. Cancer Res. 2013; 73:6711–21. [PubMed: 24072745]
9. Villa-Morales M, Fernandez-Piqueras J. Targeting the Fas/FasL signaling pathway in cancer therapy. Expert Opin Therapeut Targets. 2012; 16:85–101.
10. Scanlan MJ, Raj BK, Calvo B, Garin-Chesa P, Sanz-Moncasi MP, Healey JH, et al. Molecular cloning of fibroblast activation protein alpha, a member of the serine protease family selectively expressed in stromal fibroblasts of epithelial cancers. Proc Natl Acad Sci U S A. 1994; 91:5657–61. [PubMed: 7911242]
11. Samel D, Muller D, Gerspach J, Assohou-Luty C, Sass G, Tiegs G, et al. Generation of a FasL-based proapoptotic fusion protein devoid of systemic toxicity due to cell-surface antigen-restricted Activation. J Biol Chem. 2003; 278:32077–82. [PubMed: 12773535]
12. Bremer E, ten Cate B, Samplonius DF, de Leij LF, Helfrich W. CD7-restricted activation of Fas-mediated apoptosis: a novel therapeutic approach for acute T-cell leukemia. Blood. 2006; 107:2863–70. [PubMed: 16332967]
13. Milenic DE, Brady ED, Garmestani K, Albert PS, Abdulla A, Brechbiel MW. Improved efficacy of alpha-particle-targeted radiation therapy: dual targeting of human epidermal growth factor receptor-2 and tumor-associated glycoprotein 72. Cancer. 2010; 116:1059–66. [PubMed: 20127951]
14. Johnson VG, Schlom J, Paterson AJ, Bennett J, Magnani JL, Colcher D. Analysis of a human tumor-associated glycoprotein (TAG-72) identified by monoclonal antibody B72. 3. Cancer Res. 1986; 46:850–7. [PubMed: 3940648]
15. Molina R, Auge JM, Escudero JM, Marrades R, Vinolas N, Carcereny E, et al. Mucins CA 125, CA 19.9, CA 15.3 and TAG-72. 3 as tumor markers in patients with lung cancer: comparison with CYFRA 21–1, CEA, SCC and NSE. Tumour Biol. 2008; 29:371–80. [PubMed: 19060513]
16. Chen L, Wang Y, Liu X, Dou S, Liu G, Hnatowich DJ, et al. A new TAG-72 cancer marker peptide identified by phage display. Cancer Lett. 2008; 272:122–32. [PubMed: 18723274]
17. Zhang Y, Deng ZS, Liao MM, Wang N, Zhang XQ, Yu HY, et al. Tumor associated glycoprotein-72 is a novel marker for poor survival in hepatocellular carcinoma. Pathol Oncol Res. 2012; 18:911–6. [PubMed: 22434316]
18. Epivatianos A, Poulopoulos A, Kayavis I, Papanayotou P. Tumor-associated glycoprotein 72 (TAG-72) expression in salivary gland neoplasia: an immunohistochemical study using the monoclonal antibody (MAb) CC49. Oral Dis. 2000; 6:112–7. [PubMed: 10702789]
19. Mohsin H, Jia F, Sivaguru G, Hudson MJ, Shelton TD, Hoffman TJ, et al. Radiolanthanide-labeled monoclonal antibody CC49 for radioimmunotherapy of cancer: biological comparison of DOTA conjugates and 149Pm, 166Ho, and 177Lu. Bioconjugate Chem. 2006; 17:485–92.
20. Chan DV, Sharma R, Ju CY, Roffler SR, Ju ST. A recombinant scFv-FasLext as a targeting cytotoxic agent against human Jurkat-Ras cancer. J Biomed Sci. 2013; 20:16. [PubMed: 23497165]
21. Brandwein MS, Huvos AG, Patil J, Jagirdar J. Tumor-associated glycoprotein distribution detected by monoclonal antibody B72. 3 in salivary neoplasia. Cancer. 1992; 69:2623–30. [PubMed: 1315205]
22. Hoesel B, Schmid JA. The complexity of NF-kappaB signaling in inflammation and cancer. Mol Cancer. 2013; 12:86. [PubMed: 23915189]
23. Dhillon AS, Hagan S, Rath O, Kolch W. MAP kinase signalling pathways in cancer. Oncogene. 2007; 26:3279–90. [PubMed: 17496922]
24. Zheng HX, Cai YD, Wang YD, Cui XB, Xie TT, Li WJ, et al. Fas signaling promotes motility and metastasis through epithelial-mesenchymal transition in gastrointestinal cancer. Oncogene. 2013; 32:1183–92. [PubMed: 22508480]
25. Barnhart BC, Legembre P, Pietras E, Bubici C, Franzoso G, Peter ME. CD95 ligand induces motility and invasiveness of apoptosis-resistant tumor cells. EMBO J. 2004; 23:3175–85. [PubMed: 15272306]

26. Hoffman RM. The multiple uses of fluorescent proteins to visualize cancer in vivo. Nat Rev Cancer. 2005; 5:796–806. [PubMed: 16195751]
27. Hoffman RM, Yang M. Whole-body imaging with fluorescent proteins. Nat Protoc. 2006; 1:1429–38. [PubMed: 17406431]
28. Lee SE, Bairstow SF, Werling JO, Chaubal MV, Lin L, Murphy MA, et al. Paclitaxel nanosuspensions for targeted chemotherapy - nanosuspension preparation, characterization, and use. Pharm Dev Technol. 2014; 19:438–53. [PubMed: 23617261]
29. Ashe PC, Berry MD. Apoptotic signaling cascades. Prog Neuropsychopharmacol Biol Psychiatry. 2003; 27:199–214. [PubMed: 12657360]
30. de Carvalho-Neto PB, dos Santos M, de Carvalho MB, Mercante AM, dos Santos VP, Severino P, et al. FAS/FASL expression profile as a prognostic marker in squamous cell carcinoma of the oral cavity. PLoS ONE. 2013; 8:e69024. [PubMed: 23894399]
31. Peter ME, Budd RC, Desbarats J, Hedrick SM, Hueber AO, Newell MK, et al. The CD95 receptor: apoptosis revisited. Cell. 2007; 129:447–50. [PubMed: 17482535]
32. Igney FH, Behrens CK, Krammer PH. Tumor counterattack–concept and reality. Eur J Immunol. 2000; 30:725–31. [PubMed: 10741386]
33. O'Connell J, O'Sullivan GC, Collins JK, Shanahan F. The Fas counterattack: Fas-mediated T cell killing by colon cancer cells expressing Fas ligand. J Exp Med. 1996; 184:1075–82. [PubMed: 9064324]
34. Gastman BR, Atarshi Y, Reichert TE, Saito T, Balkir L, Rabinowich H, et al. Fas ligand is expressed on human squamous cell carcinomas of the head and neck, and it promotes apoptosis of T lymphocytes. Cancer Res. 1999; 59:5356–64. [PubMed: 10537320]
35. Sawhney M, Mathew M, Valarmathi MT, Das SN. Age related changes in Fas (CD95) and Fas ligand gene expression and cytokine profiles in healthy Indians. Asian Pac J Allergy Immunol. 2006; 24:47–56. [PubMed: 16913188]
36. Manchanda P, Sharma SC, Das SN. Differential regulation of IL-2 and IL-4 in patients with tobacco-related oral squamous cell carcinoma. Oral Dis. 2006; 12:455–62. [PubMed: 16910915]
37. Alvarez RD, Partridge EE, Khazaeli MB, Plott G, Austin M, Kilgore L, et al. Intraperitoneal radioimmunotherapy of ovarian cancer with 177Lu-CC49: a phase I/II study. Gynecol Oncol. 1997; 65:94–101. [PubMed: 9103398]
38. Sharifzadeh Z, Rahbarizadeh F, Shokrgozar MA, Ahmadvand D, Mahboudi F, Jamnani FR, et al. Genetically engineered T cells bearing chimeric nanoconstructed receptors harboring TAG-72-specific camelid single domain antibodies as targeting agents. Cancer Lett. 2013; 334:237–44. [PubMed: 22902507]
39. Hombach A, Heuser C, Sircar R, Tillmann T, Diehl V, Kruis W, et al. T cell targeting of TAG72+ tumor cells by a chimeric receptor with antibody-like specificity for a carbohydrate epitope. Gastroenterology. 1997; 113:1163–70. [PubMed: 9322511]
40. Askenasy N, Yolcu ES, Yaniv I, Shirwan H. Induction of tolerance using Fas ligand: a double-edged immunomodulator. Blood. 2005; 105:1396–404. [PubMed: 15486063]
41. Aoki K, Kurooka M, Chen JJ, Petryniak J, Nabel EG, Nabel GJ. Extracellular matrix interacts with soluble CD95L: retention and enhancement of cytotoxicity. Nat Immunol. 2001; 2:333–7. [PubMed: 11276204]
42. Schulte M, Reiss K, Lettau M, Maretzky T, Ludwig A, Hartmann D, et al. ADAM10 regulates FasL cell surface expression and modulates FasL-induced cytotoxicity and activation-induced cell death. Cell Death Differ. 2007; 14:1040–9. [PubMed: 17290285]
43. Hoffman RM. Patient-derived orthotopic xenografts: better mimic of metastasis than subcutaneous xenografts. Nat Rev Cancer. 2015; 15:451–2. [PubMed: 26422835]
44. Lin A, Karin M. NF-kappaB in cancer: a marked target. Semin Cancer Biol. 2003; 13:107–14. [PubMed: 12654254]
45. Mitsiades N, Yu WH, Poulaki V, Tsokos M, Stamenkovic I. Matrix metal-loproteinase-7-mediated cleavage of Fas ligand protects tumor cells from chemotherapeutic drug cytotoxicity. Cancer Res. 2001; 61:577–81. [PubMed: 11212252]

46. Almendro V, Ametller E, Garcia-Recio S, Collazo O, Casas I, Auge JM, et al. The role of MMP7 and its cross-talk with the FAS/FASL system during the acquisition of chemoresistance to oxaliplatin. PLoS One. 2009; 4:e4728. [PubMed: 19266094]

47. Saigusa S, Tanaka K, Ohi M, Toiyama Y, Yasuda H, Kitajima T, et al. Clinical implications of Fas/Fas ligand expression in patients with esophageal squamous cell carcinoma following neoadjuvant chemoradiotherapy. Mol Clin Oncol. 2015; 3:151–6. [PubMed: 25469286]

48. Agnihotri R, Crawford HC, Haro H, Matrisian LM, Havrda MC, Liaw L. Osteopontin, a novel substrate for matrix metalloproteinase-3 (stromelysin-1) and matrix metalloproteinase-7 (matrilysin). J Biol Chem. 2001; 276:28261–7. [PubMed: 11375993]

49. Hoffman RM, Yang M. Subcellular imaging in the live mouse. Nat Protoc. 2006; 1:775–82. [PubMed: 17406307]

50. Hoffman RM, Yang M. Color-coded fluorescence imaging of tumor-host interactions. Nat Protoc. 2006; 1:928–35. [PubMed: 17406326]

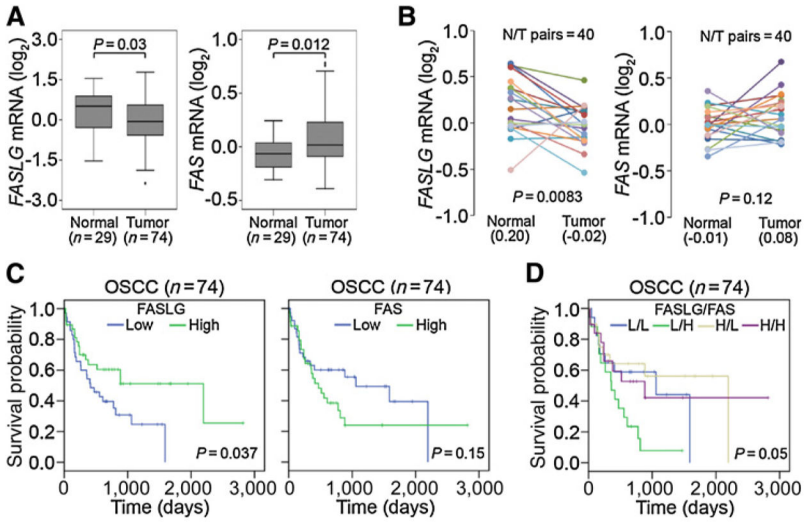

Figure 1.

Clinical relevance of the Fas ligand (FasL)/Fas ratio in OSCC. **A** and **B,** Gene expression levels of the Fas ligand (*FASLG*) and Fas (*FAS*) in unpaired (GSE42743; **A**) and paired (GSE13601; **B**) normal and tumor tissues derived from OSCC patients. Statistical significance was analyzed by a *t* test in **A** and a paired *t* test in **B. C** and **D,** Kaplan–Meier analysis of *FASLG, FAS* (**C**), and combined *FASLG*/*FAS* (**D**) gene expressions in OSCC tissues (GSE42743).

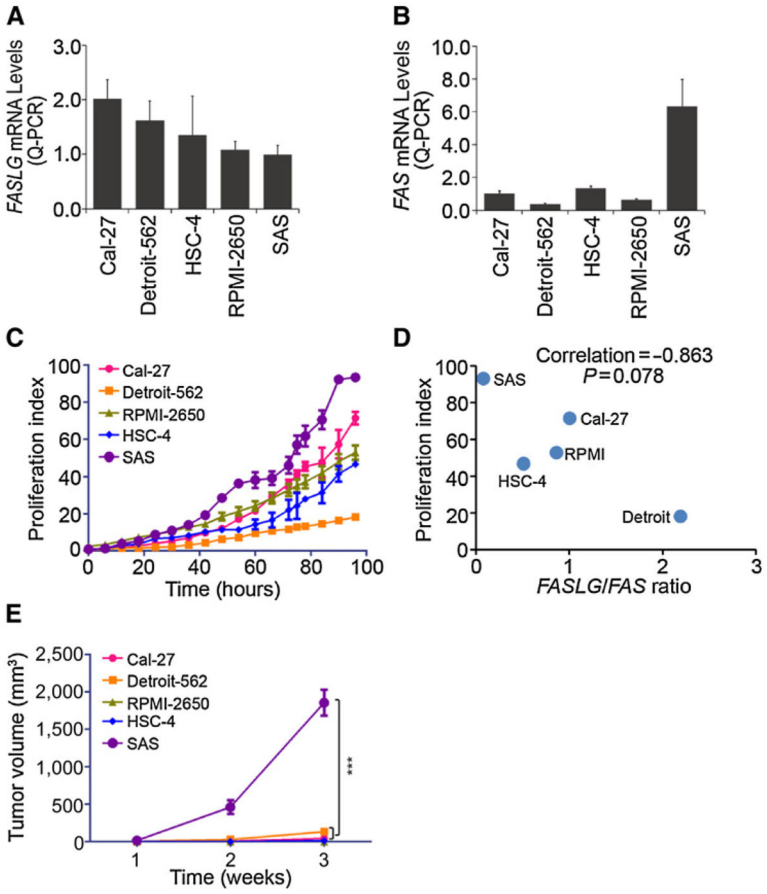

Figure 2.

A low Fas ligand (FasL)/Fas ratio promotes tumor growth of OSCC *in vitro* and *in vivo*. **A** and **B,** qPCR Analysis of *FASLG* (**A**) and *FAS* (**B**). **C,** *In vitro* cell proliferation indexes of the OSCC lines were determined with the IncuCyte Life-Cell Imaging System. **D,** Correlation between the FasL/Fas ratio and cell proliferation rate in OSCC cells. Spearman correlation coefficient = 0.863; $P = 0.078$. **E,** Tumor growth rates of the OSCC lines *in vivo*. Each of the OSCC lines were subcutaneously implanted into mice ($n = 5$). Tumor volume of each of the OSCC lines was monitored weekly. Data were presented as mean ± SE and subjected to one-way ANOVA with Tukey *post hoc* tests to analyze the statistical significances. The symbol "***" represents $P < 0.001$.

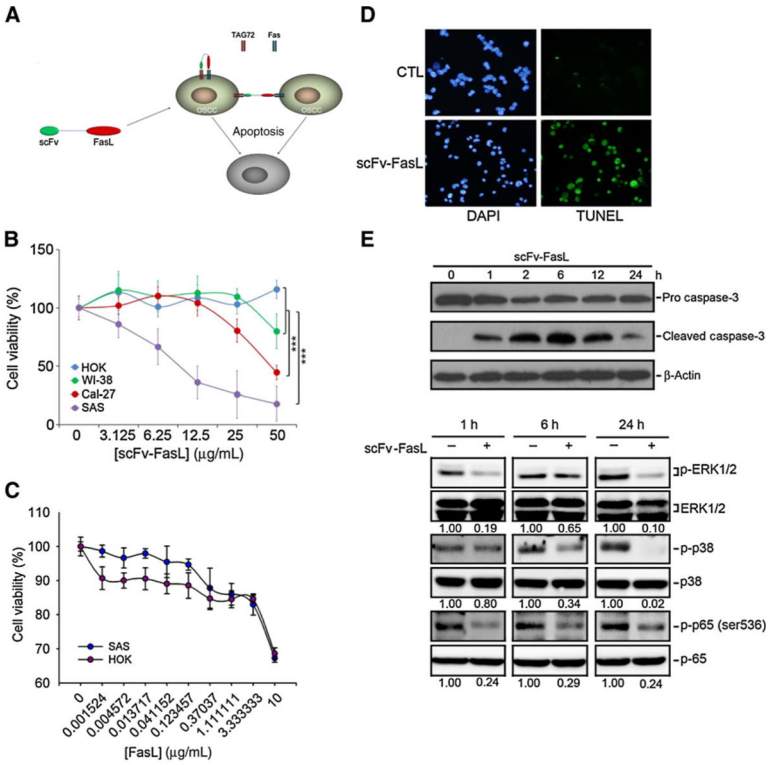

Figure 3.

The recombinant hcc49scFv-Fas ligand (FasL) effectively killed oral cancer cells with a low FasL/Fas ratio *in vitro*. **A,** The putative strategy of using recombinant hcc49scFv-FasL to kill OSCC. **B,** The killing efficacy of recombinant hcc49scFv-FasL at various concentrations on normal cell lines, HOK and WI-38, and the OSCC lines, Cal-27 and SAS. Data from three independent experiments were shown as mean ± SE. Statistical differences were analyzed by one-way ANOVA with Tukey *post hoc* tests and the symbol "***" represents $P < 0.001$. **C,** The killing efficacy of recombinant FasL at various concentrations HOK and SAS cells. Data from three independent experiments were shown as mean ± SE. **D,** TUNEL assay for SAS cells without (control, CTL) or with hcc49scFv-FasL (50 μg/mL) treatment. **E,** The cleaved caspase-3 (top) and phosphorylation levels of ERK1/2, p38, and p65 (bottom) were assessed by a Western blot analysis after treatment of SAS cells with 50 μg/mL hcc49scFv-FasL for the indicated time points. Quantitative results of p-ERK, p-p38, and p-p65 protein levels, which were respectively adjusted to their total protein levels.

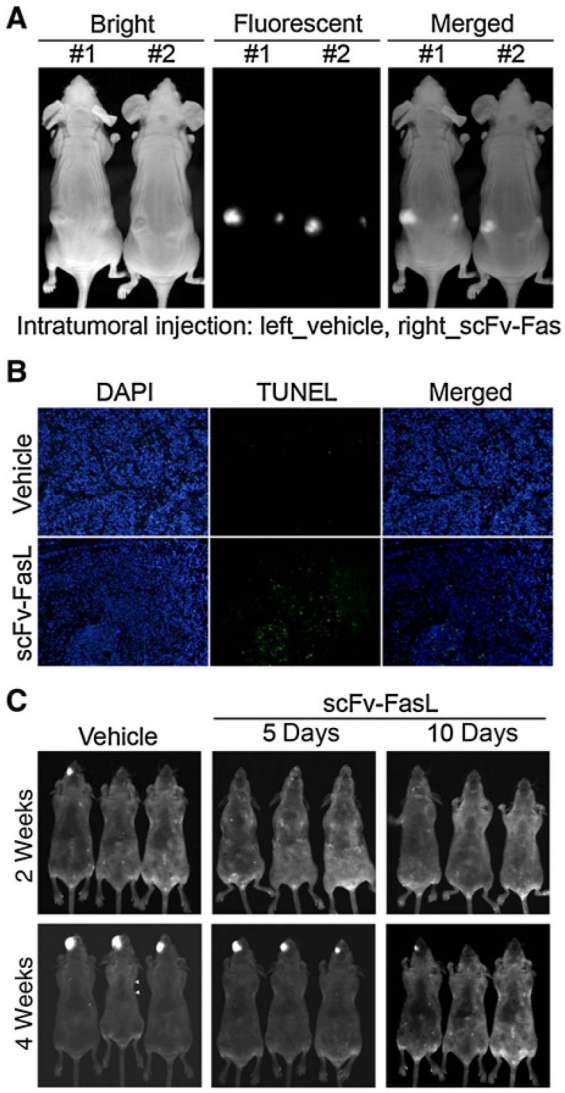

Figure 4.

The recombinant hcc49scFv-Fas ligand (FasL) dramatically inhibits tumor growth of SAS cells with a low FasL/Fas ratio *in vivo*. **A,** An intratumoral injection of hcc49scFv-FasL (1 mg) twice daily suppressed the tumor growth of SAS cells in a subcutaneous implantation model. **B,** TUNEL assay of tissues derived from a tumor of SAS cells treated without (Vehicle) or with hcc49scFv-FasL for 10 days. **C,** The intraperitoneal administration of the hcc49scFv-FasL for 5 or 10 days was capable of inhibiting the tumor growth of SAS cells in an orthotropic model of OSCC.

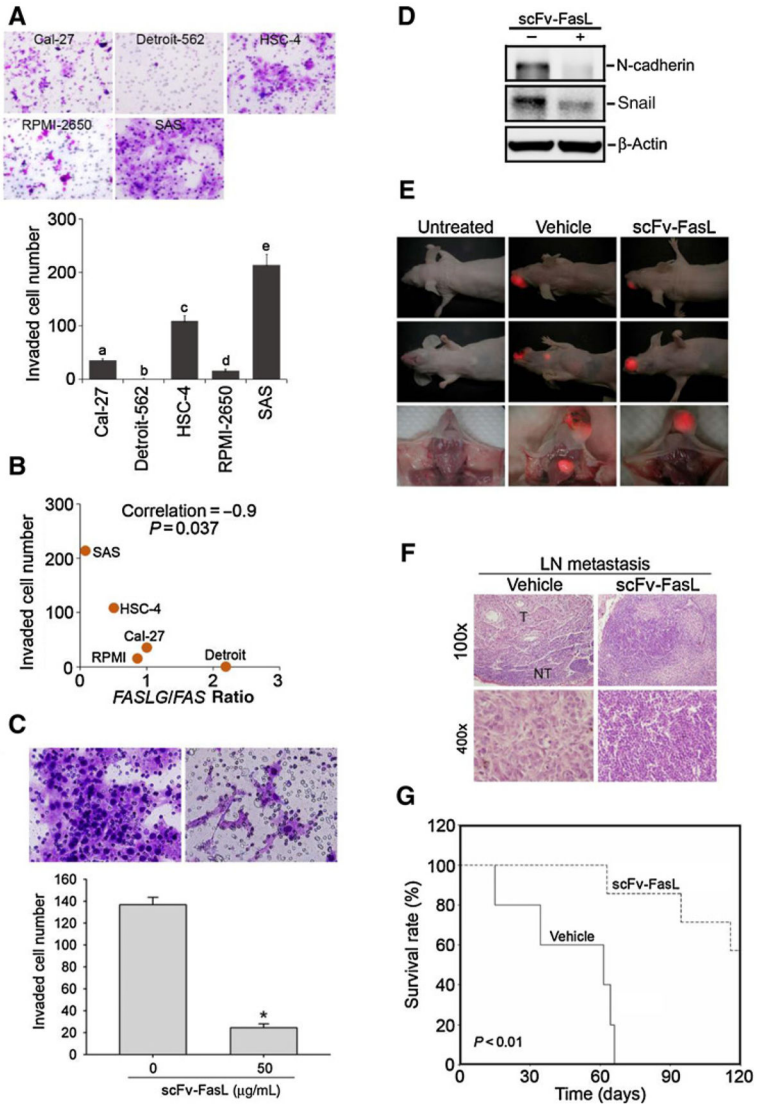

Figure 5.

The FasL/Fas ratio is inversely correlated with the invasive abilities of OSCC cells and significant antimetastatic effects of the hcc49scFv-FasL in a SAS orthotopic graft model. **A,** *In vitro* invasive abilities of OSCC cell lines. Values are presented as the mean ± SE of three independent experiments. Data were analyzed using a one-way ANOVA with Tukey *post hoc* tests at 95% confidence intervals; different letters represent different levels of significance. **B,** Correlation between the FasL/Fas ratio and the invasiveness of the OSCC cell lines. Spearman correlation coefficient = 0.9; $P = 0.037$. **C,** SAS cells were treated by the 50 μg/mL hcc49scFv-FasL for the Matrigel invasion assays. Values are presented as the mean ± SE of three independent experiments. *, $P < 0.05$ compared with the vehicle groups. **D,** Mesenchymal markers, N-cadherin, and Snail were expressed in hcc49scFv-FasL–treated SAS cells. Lysates were collected from cells cultured with or without hcc49scFv-FasL (50 μg/mL) for 24 hours and subjected to a Western blot analysis. **E,** Administration of the hcc49scFv-FasL through an intraperitoneal injection prevented the neck lymph node

metastasis of DsRed-labeled SAS cells. **F,** Neck lymph node tissues were histologic analyzed by H&E staining. Histopathology of the lymph nodes are shown at ×100 (top) and ×400 (bottom). *T,* tumor part; *NT,* nontumor part. **G,** An overall survival curve was produced for tumor-bearing mice after treatment without or with the hcc49scFv-FasL using the Kaplan–Meier method. The *P* values were determined using a log-rank test.

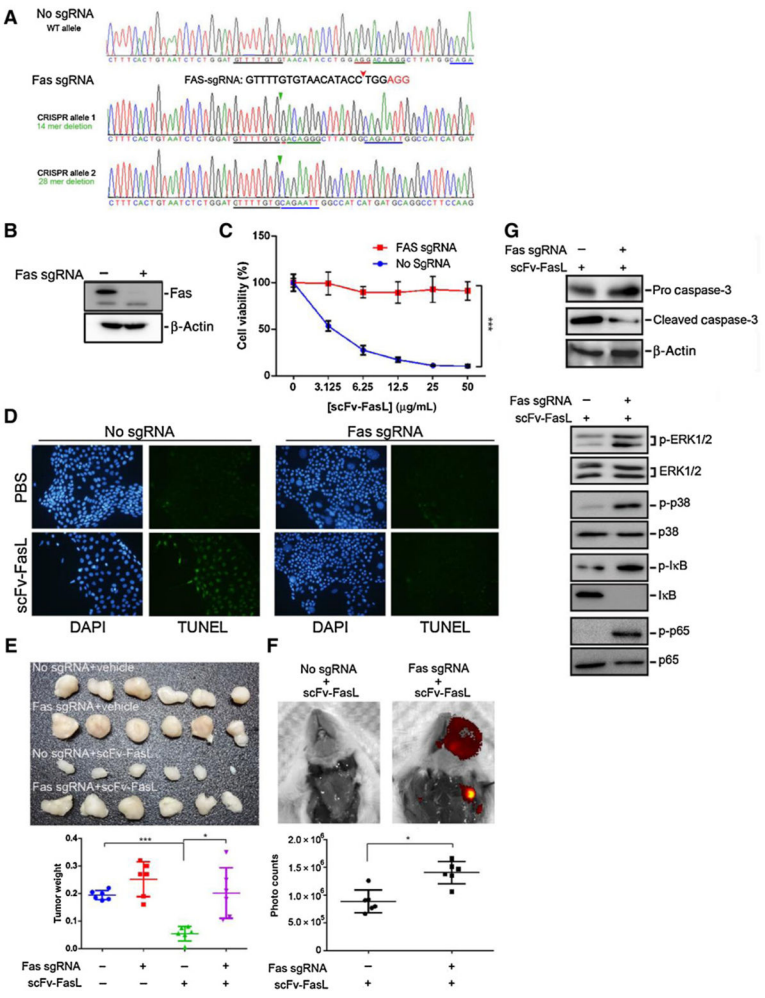

Figure 6.

Fas Crispr knockout relieves the tumoricidal efficacy of hcc49scFv-FasL on SAS cells *in vitro* and *in vivo*. **A,** Genomic DNA sequencing results of SAS cells without (no sgRNA) or with Fas (Fas sgRNA) Crispr knockout. The protospacer adjacent motif (PAM) sequence was marked in red and the red arrow indicated the cutting site of Crispr nuclease. The oligonucleotides underlined in green, blue, and black denote the original DNA sequences of Fas. **B,** Western blot analysis for Fas and β-actin protein expression in Fas-sgRNA SAS cells. **C,** The killing efficacy of hcc49scFv-FasL at various concentrations on parental (no-sgRNA) and Fas Crispr knockout (Fas-sgRNA) SAS cells. Data from three independent experiments were shown in mean ± SE. Statistical differences were analyzed by one-way ANOVA with Tukey *post hoc* tests and the symbol "***" represents $P < 0.001$. **D,** TUNEL assay for SAS cells without (no-sgRNA) or with Fas (Fas-sgRNA) Crispr knockout in the absence (PBS) or presence of hcc49scFv-FasL (50 μg/mL) treatment for 24 hours. **E,** Tumor appearance (top) and volume (bottom) of parental (no-sgRNA) and Fas Crispr knockout SAS cells in the absence or presence of the treatment with hcc49scFv-FasL (1 mg) twice daily in a subcutaneous implantation model. **F,** The distribution (top) and fluorescent intensity (bottom) of DsRed2-expressing SAS cells without (no-sgRNA) or with Fas Crispr

knockout after the treatment with hcc49scFv-FasL for 10 days in an orthotropic mouse model. Statistical differences were analyzed by Student *t* test. The symbols "*" and "***" represent $P < 0.05$ and 0.001, respectively. **G,** Western blot analysis for the protein expression of pro/cleaved caspase-3 and β-actin (top), as well as the phosphorylated and total ERK1/2, p38, IκB, and p65 (bottom), in whole-cell lysates derived from parental and Fas Crispr knockout SAS cells posttreatment with hcc49scFv-FasL at 50 μg/mL for 24 hours. In **B** and **G**, β-actin was used as an internal control of protein loading.